Order−Disorder Transitions in Cross-Linked Block Copolymer Solids

Hyeok Hahn,[†] Arup K. Chakraborty,[†,‡,§,||] Jayajit Das,[†,§] John A. Pople,[⊥] and Nitash P. Balsara[*,†,§,#]

Department of Chemical Engineering, University of California, Berkeley, California 94720; Department of Chemistry, University of California, Berkeley, California 94720; Materials Science Division, Lawrence Berkeley National Laboratory, University of California, Berkeley, California 94720; Physical Biosciences Division, Lawrence Berkeley National Laboratory, University of California, Berkeley, California 94720; Stanford Synchrotron Laboratory, SLAC, PO Box 4349, Stanford, California 94309; and Environmental Energy Technologies Division, Lawrence Berkeley National Laboratory, University of California, Berkeley, California 94720

Received July 13, 2004; Revised Manuscript Received October 12, 2004

ABSTRACT: The nature of order−disorder transitions in cross-linked diblock copolymer melts was studied using small-angle X-ray scattering (SAXS) and birefringence measurements. Experiments were conducted on cross-linked polystyrene-*block*-polyisoprene copolymer samples wherein the polyisoprene block was selectively cross-linked at a temperature well above the order−disorder transition temperature of the pure block copolymer. We find a reversible transition from a disordered gel to an ordered gel when the cross-linking density is below a critical value. The rheological properties of disordered block copolymer gels are very different from that of cross-linked homopolymer gels.

I. Introduction

The fact that molten block copolymers undergo reversible order−disorder transitions is well-established.[1,2] In the ordered state, the blocks are microphase-separated into structures with either crystalline (e.g., spheres arranged on a body-centered-cubic lattice) or liquid crystalline (e.g., cylinders arranged on a hexagonal lattice) symmetry. In the disordered state, block copolymers are isotropic liquids. Microphase separation of block copolymers is exploited in a number of practical applications such as thermoplastic elastomers and adhesives.[3−6] In these traditional applications, the microphase separation transition is used once during the lifetime of the product—the material is processed in the disordered (liquid) state and used in the ordered (soft solid) state. Our objective is to create solid block copolymer materials wherein the order−disorder transition is accessed numerous times during the lifetime of the product. This would enable the use of block copolymers in new applications that rely on reversible changes in the mechanical properties of solids such as shape memory, actuators, and artificial muscles.[7−10] The possibility of using cross-linked networks in such applications was recognized long ago.[11] Polymer networks immersed in solvents can swell and shrink reversibly in response to changes in thermodynamic potentials such as solvent quality, pH, etc.[11−13] It has proven difficult to exploit the swelling of elastomers in practical applications (e.g., artificial muscles) due to two reasons: (1) the large changes in sample volume lead to fatigue and eventual degradation of mechanical integrity, and (2) the kinetics of the phase transition is slow because it is limited by the diffusion of solvent in and out of the material.[14] It is thus desirable to design solids wherein changes in material properties do not require changes in volume or diffusion across macroscopic dimensions.

Cross-linking reactions have been used to create a variety of polymeric nanostructures. Block copolymer micelles with cross-linked shells are being considered for use as drug delivery vehicles.[15−18] Macromolecules with novel architectures such as wormlike and mushroomlike structures have been produced by a combination of block copolymer self-assembly and cross-linking.[19−21] Periodic structures formed in block copolymers and their blends have been stabilized by cross-linking.[22,23] These cross-linked structures have been used as templates for preparing nanostructured inorganic materials.[24,25] The objective of these studies[15−25] was to "fix" the nanostructures.

Our objective is to create cross-linked nanostructures that disassemble and re-form spontaneously and reversibly in response to changes in temperature. We begin with a melt of a linear polystyrene−polyisoprene diblock copolymer that exhibits an ordered phase composed of polystyrene cylinders arranged on a hexagonal lattice in a polyisoprene matrix. The ordered phase melts into a disordered liquid when heated above 114 °C. We added a cross-linking agent to the block copolymer and conducted the cross-linking reaction at 160 °C, i.e., in the disordered state. The cross-linking agent used in this study selectively cross-links the polyisoprene chains. Experimental characterization of our cross-linked block copolymers was based on swelling data, optical birefringence, and small-angle X-ray scattering (SAXS). The experiments confirm the presence of a new kind of ordered block copolymer phase formed within a cross-linked matrix. We also report the result of rheological experiments on the cross-linked block copolymer solids. Our initial findings are reported in ref 26.

II. Experimental Methods

A polystyrene−polyisoprene (SI) block copolymer was synthesized and characterized by methods described in ref 27. The weight-averaged molecular weights of the polystyrene and

[†] Department of Chemical Engineering, UCB.
[‡] Department of Chemistry, UCB.
[§] Materials Science Division, UCB.
[||] Physical Biosciences Division, UCB.
[⊥] Stanford Synchrotron Laboratory.
[#] Environmental Energy Technologies Division, UCB.
* Corresponding author.

10.1021/ma0485843 CCC: $30.25
Published on Web 01/29/2005

Table 1. Characteristics of Cross-Linked Samples

sample	DCP (wt %)	polymer vol fraction in gel ϕ	gel fraction f_{gel}	mol wt between cross-links M_c^{FE} (kg/mol)	mol wt between cross-links M_c (kg/mol)	cross-link density, x
SI[0.00]	0					
SI[0.40]	0.4	N/A				
SI[0.65]	0.65	0.049	*a*	13.4	20.6	1.00
SI[0.70]	0.70	0.037	0.471	14.1	19.1	1.08
SI[1.06]	1.06	0.075	0.736	11.5	13.1	1.57
SI[1.16]	1.16	0.083	0.803	10.9	11.6	1.79
SI[1.58]	1.58	0.139	*a*	7.3	8.5	2.43
SI[1.94]	1.94	0.146	0.875	7.0	6.9	3.00
I[1.00]	1.00	0.076	0.903	14.8	13.4	

[a] Not determined.

polyisoprene blocks were 8×10^3 and 24×10^3 g/mol, respectively, and we refer to the polymer as SI(8-24). The volume fraction of polystyrene, f, was determined to be 0.21. The ratio of the weight to number-averaged molecular weights (M_w/M_n) was estimated by gel permeation chromatography to be 1.03. The glass transition temperature (T_g) of the polystyrene microphase was determined, using a TA Instruments model 2920 DSC with a heating rate of 10 °C/min, to be 51 °C. A polyisoprene homopolymer was also synthesized by anionic polymerization. The weight-averaged molecular weight, M_w, was 48.7×10^3 g/mol (M_w/M_n was 1.01), and we refer to the polymer as I(48).

Mixtures of dicumyl peroxide (DCP) and polymer were prepared by dissolving predetermined amounts of the components in benzene. The mixture was dried first at room temperature for 20 h, followed by further drying in a vacuum oven at 70 °C for 4 h. The final DCP concentration in the mixture was determined by weighing the dry mixture. The finite vapor pressure of DCP at 70 °C led to measurable losses of DCP during sample preparation.

DCP/SI(8-24) mixtures were molded into disks with 10 mm diameter and 1 mm thickness using a Carver press at room temperature. The disk was placed in a Parr high-pressure vessel and heated for 2 h at 160 °C and 300 psi under a nitrogen blanket. This led to the formation of bubble-free cross-linked samples. All of the experiments described below were performed on the disks thus obtained. Samples are labeled according to the wt % of DCP which ranged from 0.40 to 1.94% (Table 1). Reheating the samples to 160 °C resulted in no changes in the properties of the sample as measured by the probes given below. We thus conclude that our synthesis protocol leads to complete consumption of the cross-linking reagent. We also subjected disks of homopolystyrene and homopolyisoprene to the same protocol and found that the homopolystyrene molecular weight remained unchanged, while the homopolyisoprene was converted to a cross-linked gel. It is thus obvious that our protocol results in selective cross-linking of the polyisoprene chains.

The network structure of our samples was studied by immersing them in toluene, a good solvent for both polystyrene and polyisoprene, while order−disorder transition temperatures were determined by birefringence and SAXS. Birefringence experiments were conducted on an apparatus described in ref 28. The samples were capped with fused quartz windows and placed in a thermostated oven between crossed polarizers, and the fraction of incident light power (from a Nd:YAG laser with wavelength $\lambda = 532$ nm) that was transmitted was monitored as a function of thermal history. SAXS experiments were performed on beamline 1-4 of the Stanford Synchrotron Radiation Laboratory (SSRL) using samples encased between Kapton windows. The following is the configuration of the beamline: X-ray wavelength $\lambda = 1.488$ Å, wavelength spread $\sim 1\%$, and beam diameter ~ 0.5 mm. Reciprocal space, ranging from $k = 0.076$ to 1.6 nm^{-1} (where $k = 4\pi \sin(\theta/2)/\lambda$), was probed. The samples were held inside a thermostated oven. The scattering pattern was recorded with a CCD camera and azimuthally averaged. After the subtraction of the background and empty cell scattering, the measured scattering data were converted to absolute scattering intensity using a secondary standard provided by SSRL. Rheological measurements were performed using an ARES rheometer (Rheometric Scientific Inc.) using 1 mm thick, 10 mm diameter disks. The frequency (ω) dependence of the dynamic moduli (G' and G'') were measured using a strain amplitude of 2% or less. Independent measurements over a range of strain amplitudes were made to ensure that the reported values of G' and G'' were in the linear viscoelastic regime.

III. Experimental Results

Cross-linked samples weighing about 0.02 g were immersed in excess toluene for 12 h at room temperature. Samples with DCP wt % ≤ 0.6 dissolved completely, leaving no trace of a gel. These samples also did not maintain their shape when heated in the dry state to 160 °C. Immersing samples with DCP wt % ≥ 0.65 in excess toluene resulted in the formation of a swollen gel. These samples also maintained their shape when heated in the dry state to 160 °C. We conclude that the gel point of our cross-linked samples is obtained when the DCP wt % is in the vicinity of 0.65. The polymer volume fraction in the swollen state ϕ was determined by weighing the swollen gels. We accounted for the difference in densities of toluene and SI(8-24) but ignored the volume change of mixing and loss of polymer during the swelling experiment. The values of ϕ thus obtained are given in Table 1.

After completing the swelling experiments, some of the samples were dried in a vacuum oven at room temperature for 12 h and then at 80 °C for 4 h. The gel fraction, f_{gel}, defined as the ratio of the weight of the dry sample after the swelling experiment to that before the swelling experiment, in these samples is also reported in Table 1.

According to the Flory−Erman theory (FE),[13] homopolymer networks undergoing affine deformation during swelling, ϕ, obey the relationship

$$\ln(1-\phi) + \chi\phi^2 + \phi = -\left(\frac{X}{V_0}\right)V_1\phi^{1/3}\left[1 + \frac{\mu}{X}(1-\phi^{-2/3})\right] \quad (1)$$

where χ is the Flory−Huggins interaction parameter between monomers of the polymer chain and the solvent, V_0 is the unswollen sample volume, and V_1 is the molar volume of solvent. Parameters X and μ depend on the network structure. For randomly cross-linked networks Mark and co-workers have shown that[29,30]

$$\frac{X}{V_0} = \frac{\rho(M_n/M_c - 3)}{2M_n} \quad (2)$$

$$\frac{\mu}{V_0} = \frac{\rho(M_n/M_c - 1)}{2M_n} \quad (3)$$

where ρ is the polymer density, M_n is the number-

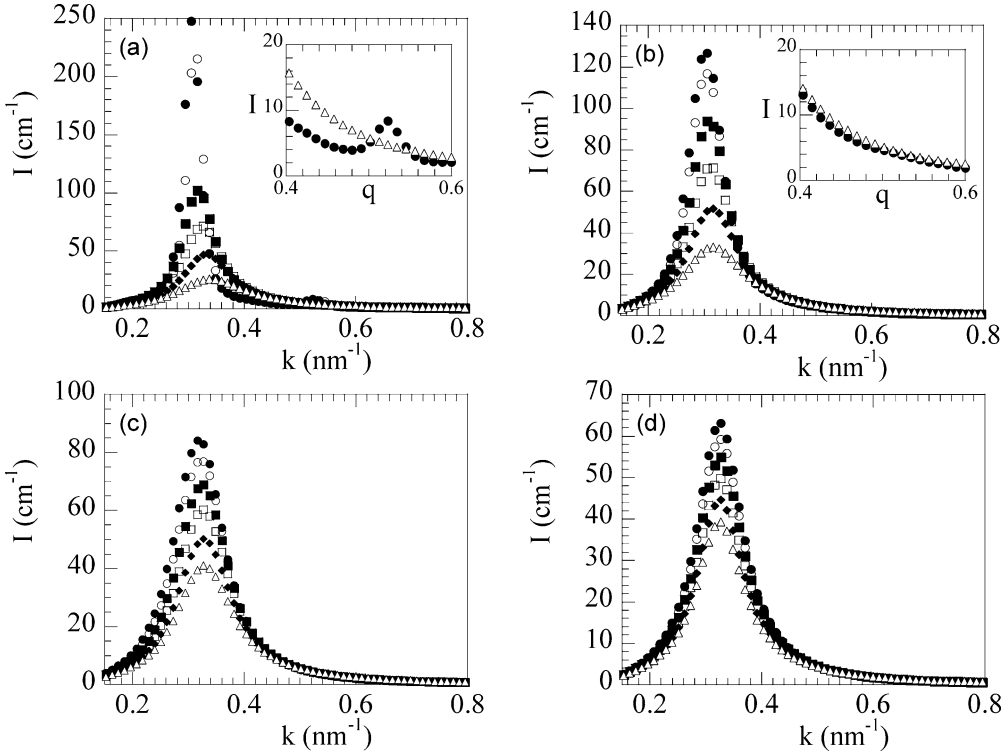

Figure 1. SAXS intensity profile $I(k)$ as a function of scattering vector k for (a) SI[0.00], (b) SI[0.65], (c) SI[1.16], and (d) SI[1.94] at different temperatures. Filled circles, 70 °C; open circles, 90 °C; filled squares, 110 °C; open squares, 130 °C; filled diamonds, 150 °C; and open triangles, 170 °C. Insets of (a) and (b) show the scattering profiles in the vicinity of the second-order peak at temperatures 70 °C (filled circles) and 170 °C (open triangles).

average molecular weight of the polymer precursor, and M_c is the molecular weight between cross-links.

Equations 1−3 are strictly applicable to randomly cross-linked homopolymers. Our system is considerably more complex because we have randomly cross-linked one of the blocks of a copolymer. Unfortunately, theories that address the swelling of cross-linked block copolymers have not yet been developed. Lacking a better alternative, we used eqs 1−3 to obtain an estimate of M_c, with the measured values of ϕ and $M_n = 32$ kg/mol. We assumed that $\chi = 0.371$, which corresponds to the volume averaged value of $\chi_{ps} = 0.41$ (polystyrene and toluene) and $\chi_{pi} = 0.36$ (polyisoprene and toluene).[31] The values of M_c thus obtained are denoted as M_c^{FE} and given in Table 1. Extensive characterization of polyisoprene networks obtained by DCP cross-linking has led to the conclusion that one cross-link per DCP molecule is obtained in the system.[32] We can thus obtain a second estimate of M_c from the DCP concentration in our samples. This estimate is called M_c and is also given in Table 1. It is clear from Table 1 that there is reasonable consistency between M_c and M_c^{FE}. Because of the many unanswered questions regarding the applicability of the FE theory to cross-linked block copolymers, we have chosen to use M_c as a measure of the cross-linking density of our samples. The results of swelling experiments on a cross-linked I(48) sample with 1.00 wt % DCP are also given in Table 1. We call this cross-linked sample I[1.00].

The cross-linking density of our block copolymer samples is quantified by a parameter x, defined by

$$x = M_{c,gel}/M_c \tag{4}$$

where $M_{c,gel}$ is the molecular weight between cross-links for the sample at the gel point which is SI[0.65]. The parameter x is thus a dimensionless measure of cross-linking density, normalized to unity at the gel point.

In Figure 1, we show typical small-angle X-ray scattering profiles, $I(k)$, obtained from our samples. We restrict attention to temperatures between 70 °C (above T_g) and 170 °C (just above the cross-linking temperature). The data were obtained as a function of increasing temperature with 10 min equilibration time at each temperature. At 70 °C, $I(k)$ from the pure block copolymer, SI[0.00], contains a primary peak at $k_m = 0.31$ nm^{-1} and a second-order peak at $k_2 = 0.53$ nm^{-1} (Figure 1a). The ratio k_2/k_m is about $\sqrt{3}$, which is in agreement with that expected from cylinders arranged on a hexagonal lattice.[33,34] The scattering profiles of SI[0.00] are sensitive functions of temperature. The primary peak scattering intensity I_m changes by a factor of 10 in our temperature window. The qualitative characteristics of $I(k)$ change abruptly when T is increased from 100 to 110 °C: the width of the primary peak increases abruptly, and the second-order peak vanishes. This is a standard signature of an order-to-disorder transition.[35−38] We thus conclude that T_{ODT} of SI[0.00] is 105 ± 5 °C.

In parts b, c, and d of Figure 1 we show $I(k)$ measured from SI[0.65], SI[1.16], and SI[1.94], respectively. We see that cross-linking suppresses the second-order scattering peak (e.g., see inset of Figure 1b). The primary scattering peak is thus the dominant feature of the SAXS profiles from our cross-linked solids. In Figure 2a we plot I_m at 70 and 170 °C as a function of cross-linking density, x, for the solid samples ($x \geq 1$). We find that I_m at 70 °C decreases with increasing x, while I_m at 170 °C increases with increasing x. The decrease in I_m at 70 °C with increasing x may reflect an increased mixing on the length scale of the ordered phase or increasing structural disorder with increasing x. The

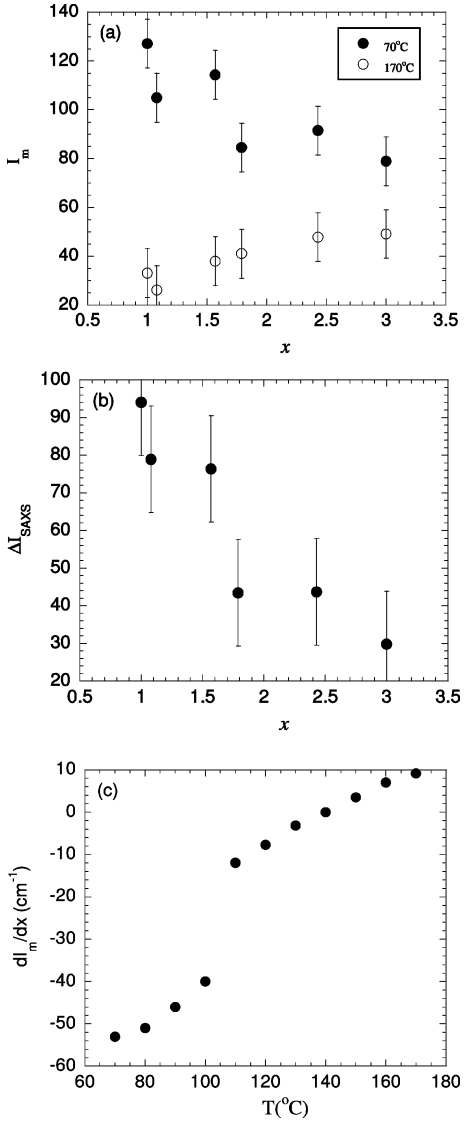

Figure 2. SAXS data from cross-linked block copolymer solids. (a) Intensity of primary SAXS peak, I_m, vs cross-linking density, x, at 70 and 170 °C. (b) Plot of ΔI_{SAXS}, the difference between I_m obtained at 70 and 170 °C, vs x. (c) Plot of dI_m/dx vs temperature T. The discontinuity in dI_m/dx occurs at a temperature that is nearly identical to the T_{ODT} of the cross-linked samples with $x \leq 1.7$.

slight increase of I_m at 170 °C with x indicates that the cross-linking brings the polyisosprene chains together and thereby increases the amplitude of the disordered concentration fluctuations. We define ΔI_{SAXS} to be the difference between I_m at 70 °C and I_m at 170 °C. It is clear from Figure 2b that ΔI_{SAXS} decreases monotonically with x, indicating that the networks become less thermally responsive as x increases. In Figure 2c we plot the slope of the least-squares linear fit through the I_m vs x data at each temperature, dI_m/dx, vs T. It is clear that dI_m/dx is a monotonically increasing function of T. This is in accordance with physical intuition. There is, however, a clear discontinuity in dI_m/dx, when the temperature is changed from 100 to 110 °C. The significance of this discontinuity will be made clear shortly.

The scattering peak at high temperatures (above 110 °C) is due to disordered concentration fluctuations. The scattering profiles from ordered phases are often expressed as a product $P(k)S(k)$, where $S(k)$ is the contribution due to the periodicity and $P(k)$ is the form factor

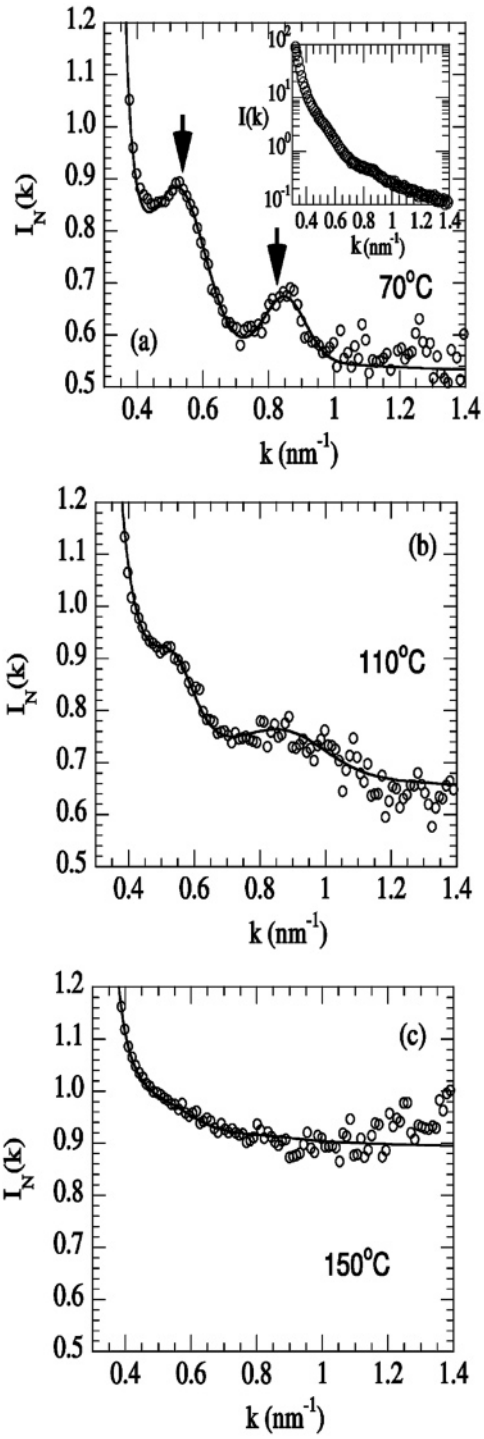

Figure 3. Normalized SAXS intensity $I_N = I/[I$ at $T = 170$ °C] vs scattering vector k from SI[0.70] in the vicinity of the second-order peak at selected temperatures (a) 70, (b) 110, and (c) 150 °C. Arrows mark higher order peaks at $\sqrt{3}k_m$ and $\sqrt{7}k_m$, where k_m is the position of the primary peak. Solid lines represent least-squares fits of the data to eq 7.

of the individual structures that are placed on the periodic lattice (e.g., cylinders). We propose a natural extension of this for periodic structures made up of chain molecules

$$I(k) = P(k)\, S(k)\, C(k) \tag{5}$$

where $C(k)$ is the contribution due to chain connectivity. $C(k)$ will become irrelevant in the strong segregation

limit (i.e., $C(k) \rightarrow 1$) where mixing between the two blocks is not permitted except in the infinitely thin interface between the microphases. It is clear, however, that our systems are far from the strong segregation limit.[2,39–41] In the disordered state, when $T \gg T_{ODT}$, $I(k)$ is dominated by chain connectivity contributions. We thus used the measured scattering profile at the highest temperature 170 °C, $I(k)_{T=170°C}$, as a measure of $C(k)$ and define a normalized scattering intensity

$$I_N(k) = I(k)/I(k)_{T=170°C} \quad (6)$$

It should be clear from the arguments given above that $I_N(k)$ will be dominated by the form factor $P(k)$ and the structure factor $S(k)$. Typical results for $I_N(k)$ are shown in Figure 3a where we show results obtained from SI-[0.70] at 70 °C. We focus on the high k region of the scattering data well beyond the primary scattering peak. The arrows represent the locations of the $\sqrt{3}k_m$ and $\sqrt{7}k_m$ peaks expected from a hexagonal lattice.[42] Plots of the normalized intensity show clear evidence of the higher order peaks corresponding to a hexagonal phase (Figure 3a). In contrast, the $I(k)$ profiles shown in the inset of Figure 3a show no clear evidence of higher order peaks.

To estimate the area under the higher order peaks, we approximate the scattering profile in the region 0.4 $nm^{-1} < k < 1.6\ nm^{-1}$ by the functional form

$$I(k) = b_1 \exp\left(-\frac{(k-b_2)^2}{b_3}\right) + c_1 \exp\left(-\frac{(k-c_2)^2}{c_3}\right) + \left(a_1 + \frac{a_2}{k-a_3}\right) \quad (7)$$

where a_1, a_2, a_3, b_1, b_2, b_3, c_1, c_2, and c_3 are fitting parameters. The first two terms in eq 7 account for the $\sqrt{3}k_m$ and $\sqrt{7}k_m$ peaks while the last term accounts for the k dependence of the background. The curve in Figure 3a is the least-squares fit of eq 7 through the data. The fitting procedure enables determination of the area under the second-order peak $A_2 = b_1\sqrt{\pi b_3}$.

Figure 3b and 3c show the effect of increasing temperature on $I_N(k)$ for SI[0.70]. It is evident that the higher order peaks diminish in intensity with increasing temperature. At 150 °C we see the higher order peaks are no longer evident (Figure 3c). The solid curves in Figure 3b,c are least-squares fits to eq 7, and they enable determination of the temperature dependence of A_2 for SI[0.70].

We obtained $I_N(k)$ from all of the block copolymer samples listed in Table 1 and estimated the temperature dependence of A_2 using eq 7 as described above. The results are shown in Figure 4a, where A_2 from different samples is plotted as a function of temperature. The finite values of A_2 obtained at temperatures ≤ 110 °C from samples with DCP wt % ≤ 1.06 clearly indicate the presence of a hexagonal ordered phase in this temperature range. Since A_2 is related to the extent of long-range order in our system, which, in turn, must depend on cross-linking density, it is no surprise that the values of A_2 depend on cross-linking density. We expect a decrease in long-range order with increasing cross-linking density. This is consistent with the trends seen in Figure 4a. A point worth noting, however, is that values of A_2 from ordered samples with DCP wt % ≤ 1.06 at a given temperature are comparable in magnitude. For example, A_2 at 70 °C from the pure block copolymer SI[0.00] is 0.058 while that from SI[1.06] at the same temperature is 0.038. This implies that the intensities of the second-order peak in $I_N(k)$ for both uncross-linked and cross-linked samples are similar. In contrast, the second-order peak is not discernable in the unnormalized $I(k)$ data shown in Figure 1 (compare parts a and b of Figure 1). Recall that our samples were made by cross-linking the disordered state at 160 °C. It is clear that when the DCP wt % ≤ 1.06 the ordered phase reappears upon cooling.

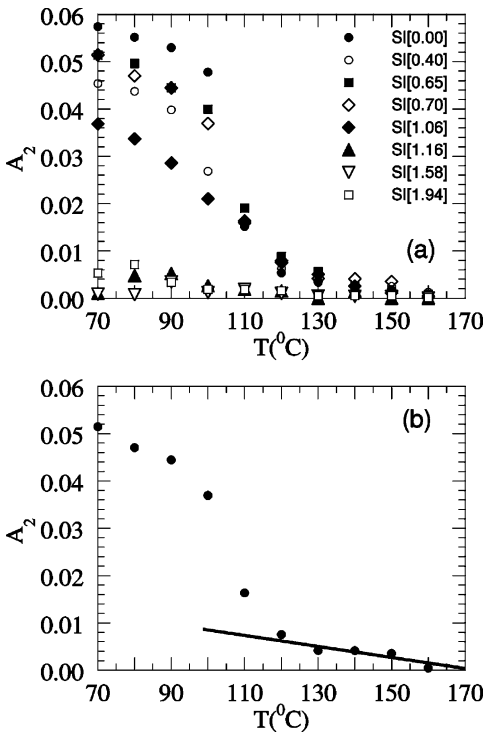

Figure 4. (a) Temperature dependence of A_2, the area under the second-order SAXS peak, obtained from cross-linked SI samples. (b) Temperature dependence of A_2 at SI[0.70]. Solid line is the least-squares fit through high-temperature data ($T \geq 130$ °C). The order−disorder transition is marked by the first point of departure from this line at $T = 110$ °C.

An abrupt change in ordering behavior is seen in Figure 4a when the DCP wt % is increased from 1.16 to 1.16. For samples with DCP wt % is ≥1.16 we see negligible values of A_2 across the entire temperature window. This implies that when the DCP wt % is ≥1.06 the ordered phase does not reappear upon cooling.

It is clear from Figure 4a that at temperatures ≥120 °C the values of A_2 for all our samples reach a "baseline" that lies between 0.01 and 0.00. Deviations from this baseline were considered as signatures of an ordered phase. Our method for determining T_{ODT} from the SAXS data is shown in Figure 4b, where we show the temperature dependence of A_2 of SI[0.70]. We fit a straight line through the high-temperature data ($T \geq 130$ °C) and identified the first point of departure from this line as the order−disorder transition. We identified T_{ODT} of all of the samples with DCP wt % ≤ 1.06 in this manner.

Birefringence measurements can also be used to detect the presence of anisotropic structures such as lamellar and hexagonal phases in block copolymers.[27,44] Figure 5 shows the temperature dependence of light intensity I leaking through our samples held between crossed polarizers, normalized by the incident intensity (I_0). We find that the temperature dependence of I/I_0, shown in Figure 5, is similar to that of A_2, shown in Figure 4a. Samples with DCP wt % ≤ 1.06 show finite

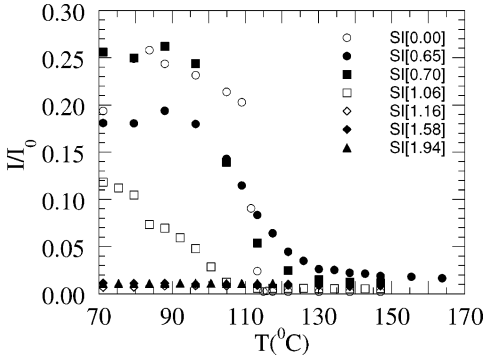

Figure 5. Temperature dependence of the birefringence signal, I/I_0, from samples with various DCP concentrations.

birefringence signals at low temperatures. In contrast, samples with DCP wt % ≥1.16 show negligible birefringence at all accessible temperatures. The birefringence signal I/I_0 from samples with DCP wt % ≤ 1.06 approach "baseline" values ranging from 0.03 to 0.00. We estimate T_{ODT} from the birefringence data using the same methodology as that described above for the SAXS data (see Figure 4b). The birefringence data confirm all of the conclusions made on the basis of the SAXS data including the effect of cross-linking density on long-range order.

In Figure 6 we show the rheological properties of our samples. We restrict our attention to temperatures between 71 °C (above T_g) and 163 °C (slightly above the cross-linking temperature). For clarity, $G'(\omega)$ and $G''(\omega)$ are shown in separate plots, without using time−temperature superposition to shift the data. The data shown in Figure 6a,b were obtained from SI[0.00]. As expected, in the low frequency limits we obtain solidlike properties (G' and G'' are insensitive functions of frequency when $T \leq 100$ °C) in the ordered state and liquidlike properties ($G' \sim \omega^2$ and $G'' \sim \omega$ when $T \geq 110$ °C) in the disordered state. The rheological properties of cross-linked samples below the gelation threshold ($x < 1$) are qualitatively similar to those shown in Figure 6a,b. Typical rheological data obtained from samples above the gelation threshold ($x \geq 1$) are shown in Figure 6c−f. It is clear that solidlike properties are obtained in both ordered and disordered states. At low frequencies in the disordered state, G' approaches a plateau due to the presence of the cross-linked network.[45] The lack of a plateau in G'' indicates the presence of polymer chains that are not attached to the network. This is consistent with the swelling data presented earlier. We use the term G_c to indicate the value of the low-frequency plateau in G' from our disordered, cross-linked samples with $x \geq 1$. In Figure 7 we show the dependence of G_c on cross-linking density, x. The circles in Figure 7 represent experimental data obtained from our cross-linked block copolymers at 163 °C. The solid curve in Figure 7 represents the shear modulus for an ideal network according to the well established theory of rubber elasticity,[45]

$$G_c^{ideal} = \rho RT/M_c \tag{8}$$

where R is the gas constant, T is temperature, ρ is copolymer density, and M_c is the average molecular weight between cross-link junctions determined by the F−E analysis (Table 1). It is assumed that ideal networks do not contain free chains. It has been

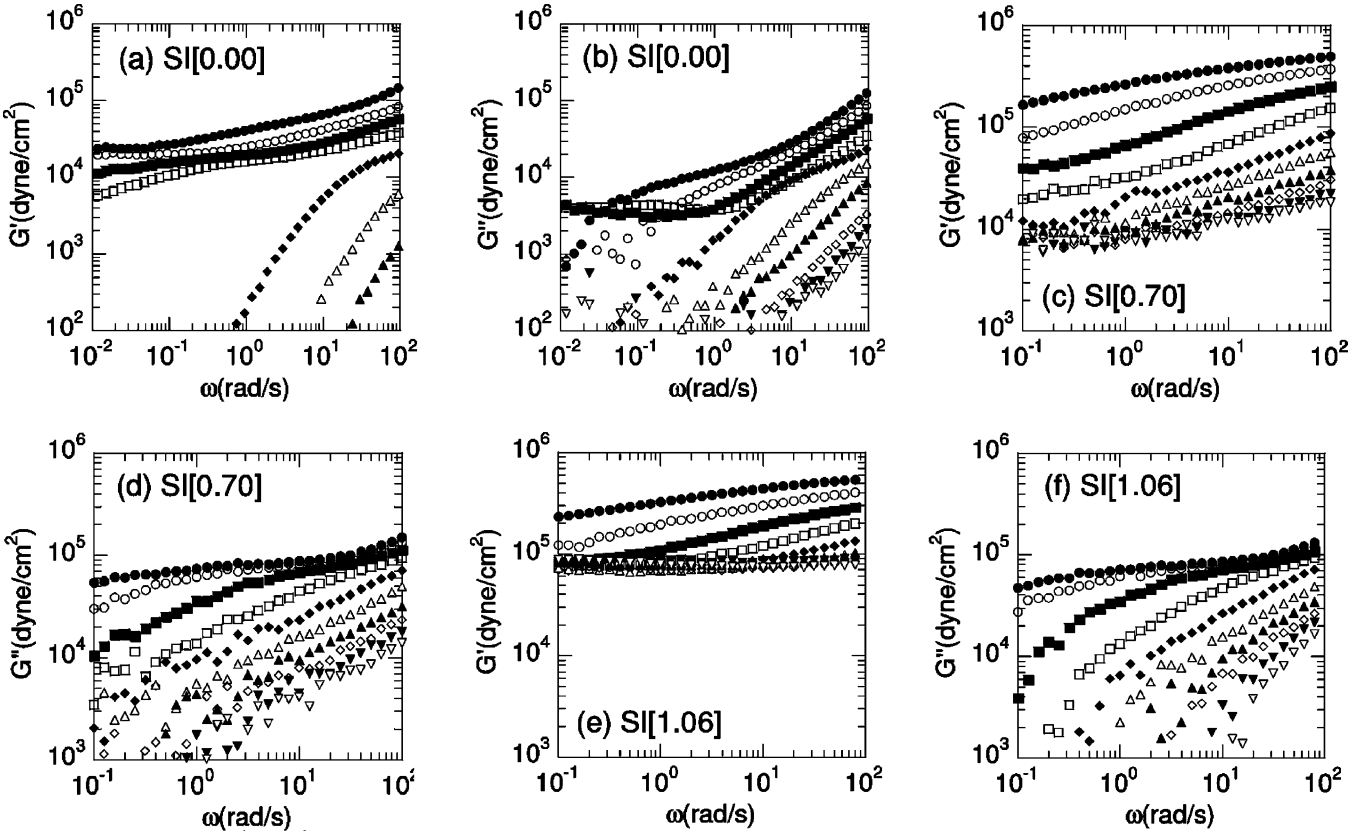

Figure 6. Shear moduli as a function of frequency, $G'(\omega)$ and $G''(\omega)$: (a, b) SI[0.00], (c, d) SI[0.70], and (e, f) SI[1.06] at various temperatures: filled circles, 71 °C; open circles, 81 °C; filled squares, 91 °C; open squares, 101 °C; filled diamonds, 112 °C; open triangles, 122 °C; filled triangles, 132 °C; open diamonds, 142 °C; filled inverted triangles, 152 °C; open inverted triangles, 163 °C.

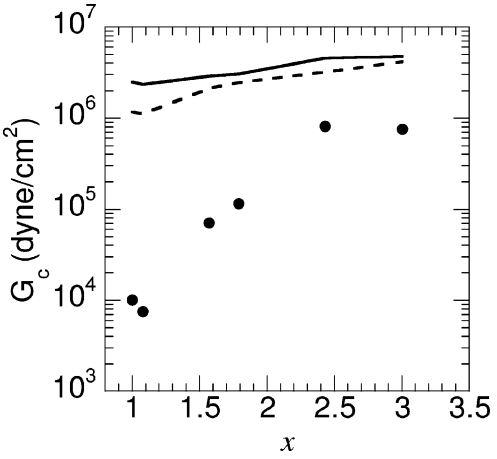

Figure 7. Plateau modulus, G_c, as a function of the cross-linking density x. Filled circles represent measured values of G_c of the cross-linked block copolymer solids. The curves show theoretical predictions of G_c. Solid curve is the ideal network model (eq 8), while the dashed curve is the nonideal network model (eq 9).

shown[46,47] that for nonideal cross-linked networks containing chains that are not bonded to the network,

$$G_c^{\text{nonideal}} = G_c^{\text{ideal}} f_{\text{gel}} \tag{9}$$

The dashed line in Figure 7 represents G_c^{nonideal} with f_{gel} values from Table 1. It is clear from Figure 7 that the cross-linked block copolymers are considerably softer than predictions based on the well-established theory of rubber elasticity. To ensure that this was not due to network imperfections, caused by our cross-linking procedure, we measured the rheological properties of the cross-linked polyisosprene homopolymer (sample I[1.00] in Table 1). The measured value of G_c was 1.5×10^6 dyn/cm^2,[48] which is in reasonable agreement with G_c^{nonideal}, calculated using eqs 8 and 9 and data given in Table 1 ($G_c^{\text{nonideal}} = 2.0 \times 10^6$ dyn/cm^2). It is thus clear that the large departure between G_c obtained from cross-linked block copolymers and that predicted by network theories is related to the structural differences between disordered cross-linked block copolymers and cross-linked homopolymers. In other words, the differences in the low-frequency mechanical properties of our samples cannot be explained by simple changes in either the average cross-linking density or gel fraction. At high cross-linking density ($x \geq 2.4$), the modulus of the cross-linked block copolymers is only a factor of 4 smaller than that of ideal networks (Figure 7). This relatively small decrease in G_c may be due to the presence of dangling ends in the cross-linked networks. The volume fraction of polystyrene (the un-cross-linked block) in our block copolymer is 21%. Thus, every chain in our networks has a dangling end composed of an 8 kg/mol polystyrene block and a polyisoprene block of variable length. At low values of x ($x \leq 2$), however, the values of G_c are smaller than those obtained from ideal network theories by factors ranging from 20 to 200 (Figure 7). Such large differences cannot be explained on the basis of changes in the length of the dangling ends. A possible reason for the unusually low values of G_c from our systems with $x \leq 2$ is the presence of "mobile" concentration fluctuations. We envision our samples to be composed on regions that are stiff (where most of the cross-linked polyisosprene chains reside) and mobile (where most of the un-cross-linked polystyrene chains reside) and that the applied strain is localized in the mobile regions. The presence of a SAXS peak in all of our samples (Figure 1) clearly indicates the presence of concentration fluctuations. One measure of the mobility of the concentration fluctuations is provided by ΔI_{SAXS}. Samples containing structures that are thermally responsive are characterized by large values of ΔI_{SAXS}, while those that have a frozen disordered state at all temperatures are characterized by a large value of ΔI_{SAXS}. It is therefore instructive to plot G_c vs ΔI_{SAXS}, as we have done in Figure 8. The data indicate an exponential decrease in G_c with increasing ΔI_{SAXS}. There thus appears to be a coupling between the thermal responsiveness of the cross-linked block copolymer solids, as gauged by the magnitude of ΔI_{SAXS}, and their mechanical responsiveness, as gauged by the magnitude of G_c. This coupling provides a new avenue for controlling the mechanical properties of cross-linked solids.

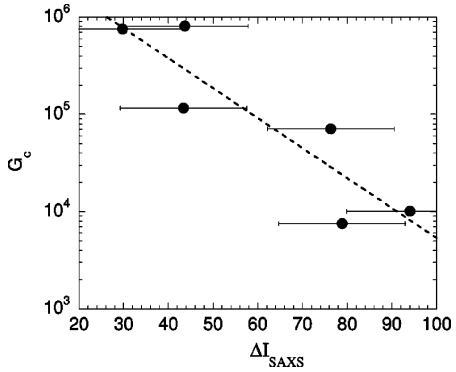

Figure 8. Low-frequency plateau modulus, G_c, vs difference between I_m obtained at 70 and 170 °C, ΔI_{SAXS}, for cross-linked block copolymer solids.

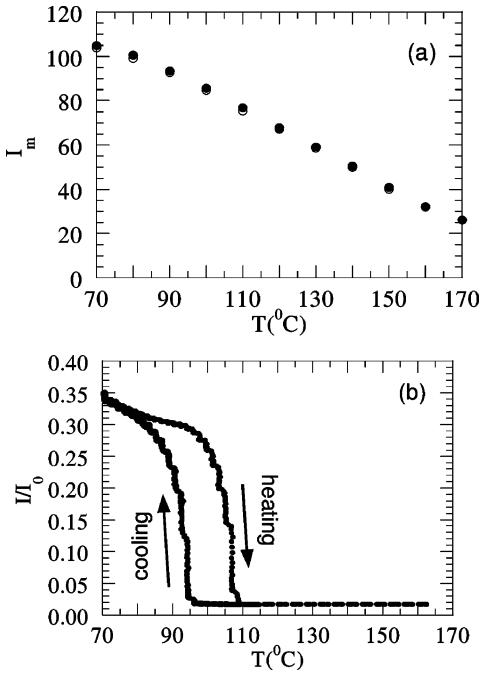

Figure 9. Temperature dependence of (a) primary SAXS peak intensity, I_m, during heating (filled circles) and cooling (open circles) of SI[0.70] and (b) the birefringence, I/I_0, during two heating and cooling cycles of SI[0.70]. In (a) the heating and cooling cycle data are almost identical.

In Figure 9a we show the temperature dependence of the primary SAXS peak intensity I_m obtained from SI[0.70] during a heating and cooling cycle. It is clear that the changes in the sample structure as seen in the

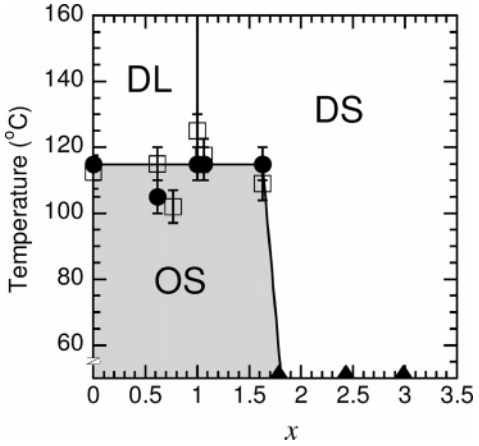

Figure 10. Phase diagram of cross-linked SI block copolymers, temperature vs x. The solid line represents experimentally determined stability limit of each phase (disordered liquid = DL, ordered solid = OS, and disordered solid = DS). The symbols represent the order−disorder transition temperature, T_{ODT}, measured by birefringence (open squares) and SAXS (filled circles). T_{ODT} of samples with $x \geq 1.7$ (filled triangles) could not be determined and are thus presumed to be below T_g.

SAXS data are reversible. In addition, there is no evidence of hysteresis in the data shown in Figure 9a. In Figure 9b we show the birefringence results obtained in heating and cooling cycles from samples SI[0.70]. It is evident that SI[0.70] must be supercooled substantially below T_{ODT} before the signatures of a fully ordered sample are obtained. The absence of hysteresis in the SAXS measurements and the presence of hysteresis in the birefringence measurements were observed in all of the samples with DCP wt % $\leq$1.06. This is due to the difference in length scales probed by the two techniques. SAXS probes the local structure on the length scale of the periodicity of the ordered phase (20 nm) while the birefringence measurements probe the structure on the length scales of the ordered grains (1 μm). The data shown in Figure 9b were obtained from two independent heating and cooling cycles. There is virtually no difference between the birefringence data obtained from the two cycles. It is thus clear that the order−disorder transitions in our solids can be accessed repeatedly and reversibly. We have thus accomplished our objective as stated in the Introduction.

In Figure 10, we show the dependence of T_{ODT} on cross-linking density x as measured by both birefringence measurements and SAXS. The phase diagram contains three kinds of phases: disordered liquids (DL) defined as samples below the gel point ($x < 1$) with negligible (I/I_0) and A_2, disordered solids (DS) defined as samples above the gel point ($x \geq 1$) with negligible (I/I_0) and A_2, and ordered solids (OS), defined as samples with finite values of (I/I_0) and A_2 regardless of x. The ordered solid is confined to a region of boxlike shape indicating the presence of two regimes: (1) a regime where T_{ODT} is essentially independent of the cross-link density (x when ≤ 1.7) and (2) a regime where ordered solids cannot be observed in our experimental window ($x > 1.7$). The triangles in Figure 10 indicate the order-disorder transition temperatures of the samples with $x > 1.7$ are below T_g, i.e., they could not be measured. The discontinuity in the dI_m/dx vs T data in Figure 2c occurs at a temperature that is nearly identical to the T_{ODT} of our cross-linked samples with $x \leq 1.7$.

To our knowledge, the fact that block copolymer chains composed of hundreds of repeat units can undergo reversible order−disorder transitions despite the attachment of one of the blocks to a cross-linked network has not been shown in previous studies.[15−25] However, liquid crystalline elastomers,[7,49−51] wherein low molar mass mesogens are covalently attached to an elastomeric network, do exhibit reversible nematic-to-isotropic phase transitions in response to changes in temperature. Considerable insight into the phase behavior of these systems has been obtained through a combination of careful synthesis, characterization, and theory.[7,49] In a closely related study Sakurai et al.[23] examined the effect of cross-linking on the morphology of a polystyrene-*block*-polybutadiene-*block*-polystyrene (SBS) copolymer. The SBS copolymer exhibited a lamellar phase in bulk at all accessible temperatures. A disordered sample was prepared by adding adequate amounts of dioctyl phthalate (DOP), a common solvent for both polystyrene and polybutadiene blocks. The polybutadiene blocks were cross-linked in the disordered state, and the DOP was then solvent-extracted to obtain a dry but cross-linked SBS sample. It was found that these cross-linked SBS samples were disordered. However, annealing these samples led to the reappearance of the lamellar phase. This study demonstrates that cross-linking does not impede order formation when the driving forces for order formation are sufficiently large. The changes in structure seen in the cross-linked SBS samples upon annealing are, however, irreversible. There was no possibility of obtaining a disordered phase in these cross-linked samples because the order−disorder transition of the block copolymer was inaccessible even in the absence of cross-links.

IV. Conclusions

We have accomplished our goal of synthesizing and characterizing cross-linked block copolymer solids that undergo reversible order−disorder transitions, thereby opening the door to applications such as shape memory materials and artificial muscles. Ordered solids were synthesized by selectively cross-linking the polyisoprene chains of a polystyrene−polyisoprene block copolymer, at temperatures well above the order−disorder transition of the pure block copolymer in the absence of cross-links. The resulting networks were characterized by swelling experiments, which gave x, the average of the cross-linking density, and birefringence and SAXS experiments which enabled the determination of the order−disorder transition temperature, T_{ODT}, as a function of x. Two regimes of behavior were observed: (1) below a critical value of x, T_{ODT} was a weak function of cross-linking density, and (2) above a critical value of x, T_{ODT} decreases extremely rapidly with cross-linking density. Rheological measurements revealed the presence of a low-frequency plateau in G' in the disordered cross-linked solids. The value of the plateau modulus is orders of magnitude lower than that obtained from homopolymers with the same cross-linking density.

References and Notes

(1) Doi, M. *Introduction to Polymer Physics*; Oxford University Press: New York, 1997.
(2) Leibler, L. *Macromolecules* **1980**, *13*, 1602.
(3) Fetters, L. J.; Morton, M. *Macromolecules* **1969**, *2*, 453.
(4) Frick, E. M.; Zalusky, A. S.; Hillmyer, M. A. *Biomolecules* **2003**, *4*, 216.
(5) Holden, G.; Legge, N. R.; Quirk, R. P.; Schroeder, H. E. *Thermoplastic Elastomer*, 2nd ed.; Hanser/Gardner: Cincinnati, OH, 1993.
(6) Yu, J. M.; Dubois, P.; Jerome, R. *Macromolecules* **1996**, *29*, 7316.

(7) Finkelman, H.; Kundler, I.; Terentjev, E.; Warner, M. *J. Phys. II* **1997**, *7*, 1059.
(8) Lendlein, A.; Langer, R. *Science* **2002**, *296*, 1673.
(9) Irie, M. *Shape Memory Polymers*; Cambridge University Press: Cambridge, UK, 1998.
(10) Liu, C.; Chun, S. B.; Mather, P. T.; Zheng, L.; Haley, E. H.; Coughlin, E. B. *Macromolecules* **2002**, *35*, 9868.
(11) Katchalsky, A. *Experientia* **1949**, *5*, 319.
(12) Tanaka, T. *Phy. Rev. Lett.* **1978**, *40*, 820.
(13) Flory, P. J.; Erman, B. *Macromolecules* **1982**, *15*, 800.
(14) deGennes, P. G. *C. R. Acad. Sci. Paris* **1997**, *324*, 343.
(15) Thurnmond, K. B.; Kowaleski, T.; Wooley, K. L. *J. Am. Chem. Soc.* **1996**, *118*, 7239.
(16) Emoto, K.; Iijima, M.; Nagasaki, Y.; Kataoka, K. *J. Am. Chem. Soc.* **2000**, *122*, 2653.
(17) Butun, V.; Billingham, N. C.; Armes, S. P. *J. Am. Chem. Soc.* **1998**, *120*, 12135.
(18) Ding, J.; Liu, G. *Macromolecules* **1998**, *31*, 6554.
(19) Zubarev, E. R.; Pralle, M. U.; Li, L.; Stupp, S. I. *Science* **1999**, *283*, 523.
(20) Ding, J.; Liu, G. *J. Phys. Chem. B* **1998**, *102*, 6107.
(21) Won, Y. Y.; Davis, H. T.; Bates, F. S. *Science* **1999**, *283*, 960.
(22) Hillmyer, M. A.; Lipic, P. M.; Hajduk, D. A.; Almdal, K.; Bates, F. S. *J. Am. Chem. Soc.* **1997**, *119*, 2749.
(23) Sakurai, S.; Twane, K.; Nomura, S. *Macromolecules* **1993**, *26*, 5479.
(24) Templin, M.; Franck, A.; Chesne, A. D.; Leist, H.; Zhang, Y.; Ulrich, R.; Schadler, V.; Wiesner, U. *Science* **1997**, *278*, 1795.
(25) Golden, J. H.; DiSalvo, F. J.; Frechet, J. M. J.; Silcox, J.; Thomas, M.; Elman, J. *Science* **1996**, *273*, 782−784.
(26) Hahn, H.; Eitouni, H. B.; Balsara, N. P.; Pople, J. A. *Phys. Rev. Lett.* **2003**, *90*, 155505.
(27) Lin, C. C.; Jonnalagadda, S. V.; Kesani, P. K.; Dai, H. J.; Balsara, N. P. *Macromolecules* **1994**, *27*, 7769.
(28) Balsara, N. P.; Perahia, D.; Safinya, C. R.; Tirrell, M.; Lodge, T. P. *Macromolecules* **1992**, *25*, 3896.
(29) Queslel, J. P.; Mark, J. E. *J. Chem. Phys.* **1985**, *82*, 3449.
(30) Queslel, J. P.; Mark, J. E. *Adv. Polym. Sci.* **1985**, *71*, 229.
(31) Gundert, F.; Wolf, B. A. In *Polymer Handbook*, 3rd ed; Brandrup, J., Immergut, E. H., Eds.; John Wiley and Sons: New York, 1989; p VII/173.
(32) Gonzalez, L.; Rodriguez, A.; Marcos, A.; Chamorro, C. *Rubber Chem. Technol.* **1996**, *69*, 203.
(33) Ryan, A. J.; Hamley, I. W. In *The Physics of Glassy Polymers*; Haward, R. N., Young, R. J., Eds.; Chapman and Hall: London, 1997.
(34) Schulz, M. F.; Khandpur, A. K.; Bates, F. S.; Almdal, K.; Mortensen, K.; Hajduk, D. A.; Gruner, S. M. *Macromolecules* **1996**, *29*, 2857.
(35) Almdal, K.; Rosedale, J. H.; Bates, F. S.; Wignall, G. D.; Fredrickson, G. H. *Phys. Rev. Lett.* **1990**, *65*, 1112.
(36) Bates, F. S.; Rosedale, J. H.; Fredrickson, G. H. *J. Chem. Phys.* **1990**, *92*, 6255.
(37) Sakamoto, N.; Hashimoto, T. *Macromolecules* **1995**, *28*, 6825.
(38) Stuhn, B.; Mutter, R.; Albrecht, T. *Europhys. Lett.* **1992**, *18*, 427.
(39) Hashimoto, T.; Fujimura, M.; Kawai, H. *Macromolecules* **1980**, *13*, 1660.
(40) Fredrickson, G. H.; Helfand, E. *J. Chem. Phys.* **1987**, *87*, 697.
(41) Helfand, E.; Wasserman, Z. R. In *Developments in Block Copolymers*; Goodman, I., Ed.; Applied Science: London, 1982; Vol. 1.
(42) The $\sqrt{4}k_m$ peak expected from a hexagonal lattice is suppressed by the cylinder form factor. The absence of the $\sqrt{4}k_m$ peak is not unexpected and is often reported in the block copolymer literature.[33,43]
(43) Koppi, K. A.; Tirrell, M.; Bates, F. S.; Almdal, K.; Mortensen, K. *J. Rheol.* **1994**, *38*, 999.
(44) Hanley, K. J.; Lodge, T. P. *J. Polym. Sci., Polym. Phys. Ed.* **1988**, *36*, 3101.
(45) Ferry, J. D. *Viscoelastic Properties of Polymers*; Wiley: New York, 1980.
(46) Langey, N. R. *Macromolecules* **1968**, *1*, 348.
(47) Graessley, W. W. In *Viscoelasticity and Flow in Polymer Melts and Concentrated Solutions* in *Physical Properties of Polymers*; Mark, J. E., et. al., Eds.; American Chemical Society: Washington, DC, 1993.
(48) The G_c of I[1.00] was determined at several temperatures ≤ 91 °C. The reported value of $G_c = (436/364)G_{c,at91°C}$ is the extrapolated modulus at 163 °C. Extrapolation based on measurements at other temperatures was within 10% of the reported value.
(49) Warner, M.; Terentjev, E. *Prog. Polym. Sci.* **1996**, *21*, 853.
(50) Mitchell, G. R.; Davis, F. J.; Guo, W.; Cywinski, R. *Polymer* **1991**, *32*, 1347.
(51) Finkelman, H.; Koch, H. J.; Rehage, G. *Makromol. Chem. Rapid Commun.* **1981**, *2*, 317.

MA0485843